POLISH HEART JOURNAL

Kardiologia Polska
The Official Peer-reviewed Journal of the Polish Cardiac Society since 1957

Online first
This is a provisional PDF only. Copyedited and fully formatted version will be made available soon

ISSN 0022–9032 e-ISSN 1897–4279

Assessment of atrial and ventricular mitral annular disjunction using cardiac computed tomography

Authors: Agata Krawczyk-Ożóg, Jakub Batko, Artur Dziewierz, Jakub Hołda, Kacper Jaśkiewicz, Barbara Zdzierak, Daniel Rams, Jakub Rusinek, Stanisław Bartuś, Mateusz K Hołda

Article type: Original article

Received: July 1, 2024

Accepted: September 2, 2024

Early publication date: September 6, 2024

Assessment of atrial and ventricular mitral annular disjunction using cardiac computed tomography

Short title: Mitral annular disjunction in CT imaging

Agata Krawczyk-Ożóg[1, 2], Jakub Batko[1], Artur Dziewierz[2, 3], Jakub Hołda[1], Kacper Jaśkiewicz[1], Barbara Zdzierak[2], Daniel Rams[1], Jakub Rusinek[1], Stanisław Bartuś[2, 3], Mateusz K Hołda[1, 4]

[1]HEART — Heart Embryology and Anatomy Research Team, Department of Anatomy, Jagiellonian University Medical College, Kraków, Poland
[2]Clinical Department of Cardiology and Cardiovascular Interventions, University Hospital, Kraków, Poland
[3]2nd Department of Cardiology, Jagiellonian University Medical College, Kraków, Poland
[4]Division of Cardiovascular Sciences, The University of Manchester, Manchester, United Kingdom

Correspondence to:
Agata Krawczyk-Ożóg, MD, PhD,
Department of Anatomy,
Jagiellonian University Medical College,
Kopernika 12; 31–034 Kraków,
phone: +48 12 422 95 11,
e-mail: krawczyk.ozog@gmail.com

WHAT'S NEW?

Three-dimensional cardiac computed tomography emerges as a reliable tool for the precise detection and assessment of both types of mitral annular disjunctions, that are located on the entire circumference of mural mitral leaflet and commissures. Among 250 patients, atrial mitral annular disjunction was identified in 25.6% and ventricular mitral annular disjunction in 27.6%. Comprehensive morphometric evaluation of MADs could prove pivotal in understanding their clinical implications.

ABSTRACT

Background: Mitral annular disjunction (MAD) is a spatial displacement of the leaflet hinge line towards the left atrium (a-MAD) or left ventricle (v-MAD).

Aims: We sought to determine morphological characteristics of MAD types along the mural mitral leaflet and commissures using cardiac computed tomography (CT) imaging.

Methods: CT images from 250 adult patients were analyzed. A three-dimensional reconstruction of the left atrial wall-mitral annulus-left ventricular wall junction was performed for the detection of MADs and their measurements.

Results: The a-MAD was identified in 25.6% of patients (12.8% of mural leaflets and 14.0% mitral commissures), while v-MAD in 27.6% of patients (23.6% of mural leaflets and 4.8% mitral commissures). Notably, the P2 scallop was the most common site for both a-MAD (10.8%) and v-MAD (22.4%). The median disjunction height and length was larger for MADs located in leaflets than commissures (all P <0.001). No significant sex-based disparities in the presence of both a-MADs and v-MADs were found. Patients with a-MAD were younger (P = 0.006) in comparison to v-MAD and no-MAD group. No differences in body mass index, body surface area, and comorbidities across the study groups (all P >0.05).

Conclusions: Cardiac CT emerges as a reliable tool for the precise detection and assessment of MADs, which are relatively frequent variations in the structure of the mitral valve annulus. MADs are typically sectional and do not extend beyond one of the mural mitral leaflet scallops or commissures. Further investigations are warranted to establish the clinical implications of a-MADs and v-MADs.

Key words: computed tomography, mitral annular disjunction, mitral annulus, mitral valve, mitral valve pathology

INTRODUCTION

Mitral annular disjunction (MAD) is defined as a discernible spatial displacement of the leaflet hinge of the mural (posterior) mitral leaflet or mitral commissures beyond the plane of the aligned atrial wall-mitral annulus-ventricular wall junction [1–3]. Two different types of MAD may be distinguished: atrial MAD (a-MAD), which is an annular displacement shifted toward the left atrium[1], and ventricular (v-MAD), which is shifted toward the left ventricle [4].

The first description of the displacement of the mitral annulus was featured in "Handbuch der systematischen Anatomie des Menschen" by Henle in 1876 [5]. Nearly a century later, in 1986, Hutchins et al. [6] thoroughly described a-MAD type based on analysis

of a large sample of autopsy specimens, hypothesizing that a-MAD is an anatomical variant of the mitral annulus that may be associated with a mitral leaflet prolapse. For many years, a-MAD was overlooked and considered clinically insignificant. However, recent studies have raised possible clinical implications of a-MAD, including its association with mitral valve disease, ventricular arrhythmias, and sudden cardiac death [7–17]. Interestingly, apart from the well-known a-MAD, a study by Hutching et al. [6] also called the other variant of mitral annulus morphology, where 'the atrium-valve junction attached well below the atrial aspect of the ventricle'. In the following decades, the second type of MAD (displacement towards the ventricle) was never again named or described. In our recent autopsy study, we have confirmed the presence of v-MAD in the population of healthy human hearts and characterized its morphology [4]. Nevertheless, the clinical significance of the v-MAD type remains uncertain.

MAD can be assessed through various imaging modalities, such as echocardiography, computed tomography (CT), and magnetic resonance (MR) imaging [8, 10–12, 18–25], with CT offering the advantage of detailed, high-resolution evaluation of the entire circumference of the mitral valve annulus [22, 23, 26]. In this study, we sought to determine the prevalence and morphological features of both a-MAD and v-MAD using three-dimensional reconstructions of the cardiac CT images.

MATERIAL AND METHODS

This study was approved by the Bioethical Committee of the Jagiellonian University Medical College in Krakow, Poland (No 1072.6120.169.2022) and adhered to the ethical guidelines of the 1964 Declaration of Helsinki.

Study population

We conducted a retrospective review of contrast-enhanced, electrocardiogram-guided cardiac CT scans from 274 consecutive patients, performed between February 2014 and November 2019 in the Clinical Department of Cardiology and Cardiovascular Interventions at University Hospital, Krakow. After an initial quality check of the scans and the exclusion of patients with poor-quality scans or a history of mitral valve replacement or repair, 250 patients (56.8% female, mean [standard deviation] age 73.9 [14.7] years) were included and subjected to further analyses. The patients underwent cardiac CT for the evaluation of various cardiovascular conditions, including aortic valve stenosis (168 patients), coronary artery disease without structural heart disease (74 patients), and assessment of coronary arteries in patients with heart failure (2 patients), mitral regurgitation (1 patient), partial anomalous pulmonary venous return

(1 patient), atrial septal defect (2 patients), left atrial myxoma (1 patient), and coronary artery anomalies (1 patient). Comprehensive chart reviews were performed to gather demographic details and past medical history for all participants.

Cardiac computed tomography

Cardiac CT scans were conducted using a 64-row dual-source scanner (Aquilion 64, Toshiba Medical Systems, Tokyo, Japan), with collimation set at 2 × 32 × 0.6 mm and temporal resolution at 165 ms. Contrast agent was injected at a dose of 1.0 ml/kg body weight and a rate of 5.5 ml/s, followed by a 40 ml saline flush at the same rate. The 30% phase of a multiphasic reconstruction (10% to 100%) was assessed as the end-systolic phase of the left ventricle and further examined. Semi-automatic segmentation of the left atrium, left ventricle, and mitral valve apparatus was performed at predefined end-systolic and end-diastolic phases using specialized three-dimensional reconstruction and visualization software (Mimics Innovation Suite 24, Materialize, Plymouth, MI, US). Three dimensional and multiplanar reconstructions were reviewed and independently evaluated by a minimum of two researchers, who were blinded to the patients' clinical backgrounds.

Definitions and measurements

The relationships between the left atrial myocardium, left ventricular myocardium, mitral valve mural leaflet, and mitral valve commissures were assessed to detect MAD in both the end-systolic and end-diastolic phases using multiplanar reconstructions. The classical arrangement of mitral valve hinge line (no-MAD) was detected when the mitral annulus insertion point was located at the border between the atrial, and ventricular myocardium and no significant displacement of the mitral leaflets hinge line toward either the left atrium or the left ventricle was present (displacement <2 mm). The v-MAD was defined as a spatial displacement of the mitral hinge line toward the left ventricle (displacement ≥2 mm) (Figure 1A–C). The a-MAD was noted when a spatial displacement of the mitral hinge line toward the left atrial wall (displacement ≥2 mm) was visible (Figure 1D–F).

If a-MAD or v-MAD were discovered, their localization within the mural mitral leaflet or commissures were precisely described. The mural part of the mitral annulus was divided into parts based on mitral valve leaflets anatomy: P1, P2, and P3 scallops, inferoseptal, and superolateral commissures [27]. Disjunction height was measured as the maximal distance between the mitral valve hinge line and the top of the left ventricular myocardium (towards the left atrium or ventricle). The disjunction length was measured as a curved line along the mitral

annulus, from the beginning to the end of MAD. These linear measurements were obtained using virtual calipers in the end-systolic phase in multiplanar reconstructions.

Statistical analysis

Data analysis was carried out using IBM SPSS Statistics 29.0 (Predictive Solutions, PA, US). Categorical variables are presented as numbers (n) and percentages. Quantitative variables are presented as means with corresponding standard deviation or median with lower and upper quartiles. Data distribution was explored with the Shapiro–Wilk test. Differences between normally distributed quantitative parameters were evaluated with Student's t-test, while non-normally distributed quantitative data were analyzed using the Mann–Whitney U test. Differences between categorical variables were determined using the χ^2 test of independence or Fisher's exact test if the number of observations in one category was below five. For multiple comparisons, the non-parametric Kruskal–Wallis test with *post hoc* Dunn test and Bonferroni correction were applied to compare values between groups. A *P*-value of <0.05 was considered statistically significant.

RESULTS

The a-MAD was identified in 25.6% of the study population, predominantly affecting only the mural leaflet (11.6%), only superolateral commissure (8.8%), or inferoseptal commissure (4.0%). In a small subset (1.2%), a-MAD was present in both the mural leaflet and one of the commissures. The v-MAD was detected in 27.6% of patients, primarily within only the mural leaflet (22.8%), with less frequent involvement of the superolateral (2.4%) or inferoseptal (1.6%) commissure; a combined presence in the mural leaflet and a commissure was note in 0.8% of cases (Table 1). The occurrence of MADs varied across different segments of the mural mitral leaflet, with the P2 scallop being the most common site for both a-MAD (10.8%) and v-MAD (22.4%) as shown in Table 1 and Figure 2. MADs were seldom found in external scallops (P1, P3). The disjunction was observed along the entire mural mitral leaflet in three cases (1.2%) (one case of v-MAD and 2 cases of a-MAD). There were no instances where both a-MAD and v-MAD co-existed in the same heart.

The median (IQR) disjunction height and length of a-MAD were larger in the mural leaflet than in the commissures (height: 5.0 [2.8–8.2] vs. 2.9 [2.2–3.4] mm; length: 10.1 [7.1–12.3] vs. 3.7 [2.8–6.2] mm; both *P* <0.001). The same relationship was observed for v-MAD for both disjunction height (5.3 [3.2–7.0] vs. 3.1 [2.5–4.1] mm; *P* <0.001) and length (12.9

[8.7–14.9] vs. 4.7 [3.3–6.5] mm; *P* <0.001). However, no differences were found between the dimensions of a-MADs and v-MADs (*P* >0.05).

The prevalence of a-MAD and v-MAD did not differ between women and men (a-MAD: males 26.2% vs. females 25.2%; *P* = 0.86; v-MAD: males 30.8% vs. females 25.2%; *P* = 0.32) (Table 2). Morphometric analyses of the 2 MAD types revealed no significant sex differences, except for a longer a-MAD disjunction in males compared females (11.4 [10.1–13.7] vs. 7.7 [6.6–11.5] mm; *P* =0.02) (Table 2).

Clinical characteristics of patients, categorized by MAD type (Table 3), showed that those with a-MAD were significantly younger than those with v-MAD and no-MAD and less frequently had severe aortic valve stenosis. There were no significant differences in body mass index, body surface area, or the presence of other comorbidities across the three groups (Table 3). Notably, one a-MAD patient experienced sudden cardiac arrest due to ventricular fibrillation. This patient also had mitral valve prolapse with intermediate mitral regurgitation but no other diseases. Cardiac arrest also occurred in two other patients, one without MAD and another with v-MAD, both due to myocardial infarction.

DISCUSSION

In this study, we demonstrated the utility of cardiac CT for detecting and evaluating MAD. The prevalence of a-MADs and v-MADs in the current study was comparable with our recent autopsied studies [1, 4], which indicates the excellent MAD detection performance of cardiac CT. Importantly, no co-existence of the a-MAD and v-MAD within the same heart was detected, which is also consistent with our previous autopsied observations (0.45% coexistence of both MAD types in the same heart) [4], suggesting distinct pathophysiological origins for these two types of MAD. Defining MAD precisely remains a challenge, especially regarding the minimum displacement necessary to classify a fragment of the mitral annulus as disjunctive [1, 2, 4]. Diagnostic criteria vary across different imaging modalities. For instance, in transthoracic echocardiography, a misalignment ≥2 mm measured in systole was sufficient to diagnose the presence of a-MAD [8, 25]. In transesophageal echocardiography, MAD was diagnosed if there was a wide separation of ≥5 mm in two-dimensional [18, 28] and three-dimensional studies [10]. For the cardiac MR or cardiac CT imaging, previous studies do not indicate any cut-off point, defining any displacement of the mitral leaflet hinge line as MAD, or using a 1 mm threshold [12, 20–24]. In our previous autopsied studies we arbitrarily chose the 2 mm cut-off point for a MAD detection (both a-MAD and v-MAD) [1, 4]. Considering the complex morphological structure of the mitral annulus, macroscopic and microscopic features

of disjunctions we have previously observed and spatial resolution of available imaging modalities we advocate for a ≥2 mm displacement as the criterion for MAD in both clinical and research settings.

The question of whether MADs represent normal anatomical variations or pathological entities, and what the clinically significant MAD height cutoff point is, remains open Unfortunately, nothing is known about the clinical significance of the v-MAD and the implications of a-MAD are not entirely clear. The a-MAD is frequently found in patients diagnosed with mitral valve prolapse and is believed to be closely associated with advanced myxomatous degeneration [8, 14]. It is even hypothesized that the floppy mitral valve develops from hypermobility of the valve apparatus, secondary to disjunction [6]. However, at the same time, attention should be paid to a vast number of patients with a-MAD present but without a myxomatous mitral valve of leaflet prolapse [1]. A systematic literature review by Bennet et al. [7] highlighted the link between ventricular arrhythmias and a-MAD. Notably, the incidence of ventricular arrhythmias was found to be higher with a greater extent of a-MAD height and circumferential area (length) [7, 12]. Furthermore, a-MAD may be associated with ventricular arrhythmias independent of concomitant mitral valve prolapse, suggesting that a-MAD itself may play a crucial role in arrhythmogenesis [12]. Conversely, Essayagh et al. concluded that the presence of a-MAD was not associated with increased mortality within the first 10 years after its diagnosis [14]. However, this does not diminish the importance of vigilant monitoring for arrhythmias in individuals identified with MAD. Finally, recognizing MAD, whether atrial or ventricular, seems crucial for patients undergoing mitral valve surgery. In patients with annular disjunctions, modifying the surgical technique may be necessary to avoid prosthetic valve replacement and ensure an optimal and long-lasting outcome of the repair [18, 19].

The incidence of a-MAD in previous clinical studies varies depending on the patient population, imaging modality, and the criteria of for defining a-MAD [29, 30]. The most common noninvasive imaging modality to detect MAD is transthoracic echocardiography. The prevalence of a-MAD identified through routine echocardiography is considerably lower than observed in autopsy studies, estimated at 9%, with a mean disjunction height of 3.5 mm [1, 8]. Assessment of MAD with echocardiography can be hampered by reduced image quality, atrial fibrillation, or myocardial infarction affecting the mitral annulus region adjacent to the left ventricle [8, 22]. Furthermore, standard echocardiography does not allow for a reliable assessment of the entire circumference of the mitral annulus, making the detection of typically small and localized MADs challenging. In contrast, three-dimensional imaging modalities allow examination of the entire circumference of the mural mitral leaflet and both commissures,

therefore should be preferably used over two-dimensional transthoracic echocardiography to assess the atrial wall-mitral annulus-ventricular wall junction [15].

Previous studies have investigated a-MAD with cardiac CT and MR imaging, which are integral to contemporary clinical diagnostics [11, 12, 21–24, 31]. These modalities allow for three-dimensional mitral annulus assessment and provide excellent morphological information on its structure [22–24, 26, 32]. Cardiac CT is a standard imaging examination performed in many patients as part of the cardiac diagnostic workup and is becoming increasingly popular. CT allows perfect spatial assessment of the mitral valve apparatus, including leaflets and annulus, with very high accuracy, without necessitating specialized protocols for MAD evaluation [32]. Although cardiac MR also allows for accurate imaging of the mitral valve annulus, it demands specific planning and protocol adjustments during data acquisition, generally yielding lower spatial resolution compared to CT [33]. The priority of cardiac MR over CT allows for the assessment of mitral regurgitation and, more importantly, late gadolinium enhancement, which is crucial in patients with MAD. As mentioned above, MAD is associated with hypermobility of the atrioventricular junction, which leads to excessive local contraction and stretching of cardiomyocytes. This can result in potential remodeling and fibrosis of the myocardium, visible as late gadolinium enhancement on MR imaging [9, 11, 24]. It is believed that the increased force applied to the weakened myocardium leads to arrhythmias, with the disjunction itself, rather than the prolapse, being responsible for the excessive mobility [11, 17, 24]. Nevertheless, both above-mentioned imaging modalities require a deep understanding of mitral valve anatomy and careful interpretation to avoid diagnostic errors. The current study showed that proper mitral annulus evaluation in CT can find MAD with similar accuracy to autopsy studies. On the contrary, in a study by Toh et al. [23] based on CT images of 98 patients, the a-MAD was identified in 96.0% of structurally normal hearts, with double peaks at bilateral sides of commissures on the prevalence distribution map. In another large-scale study by Zugwitz et al. [24] that used MR imaging, the disjunction was detected in 76% of patients, also displaying a similar type of bimodal distribution. Such discrepancies may result from erroneous overidentification of MAD in external parts of both commissaries. It is vital to properly define the boundaries between commissures and aortic (anterior) mitral leaflets to avoid overdiagnosis of MAD. The attachment point of the aorto-mitral continuity to the base of the left ventricular wall may resemble in its structure the a-MAD and therefore lead to a false diagnosis [1, 2].

Another issue worth discussing is the presence of so-called pseudo-MAD. When assessing the presence of MAD in clinical imaging, it is crucial to evaluate the diastolic phase

of the cardiac cycle to avoid potential misdiagnosis. A common error is pseudo-MAD, where the leaflet insertion is normal, but the juxtaposition of the mural leaflet and atrial wall creates the appearance of MAD. True MAD should be identified exclusively in the diastolic phase, where the leaflet hinge is visible and accurately positioned at the atrioventricular junction [34]. The use of an inappropriate imaging phase can lead to misdiagnosis. In our study, we performed segmentation during both the end-systolic and end-diastolic phases to detect MAD. All subsequent measurements were done in the end-systolic phase.

Limitations

The present study has several limitations. Firstly, it is based on data from a single institution, which may limit the generalizability of the findings. Secondly, the patient cohort comprises individuals who underwent cardiac CT primarily for the evaluation of coronary artery disease or as a prerequisite for transcatheter aortic valve implantation, among other reasons. This selection bias suggests the need for further research involving a broader spectrum of patients, especially those with mitral valve disorders and a variety of cardiac arrhythmias, to fully understand the prevalence and implications of MAD. The study analyzed CT scans performed between February 2014 and November 2019, ensuring that all included scans were technically accurate, with the mitral annular region clearly visible. Only univariate statistical analyses were performed. Additionally, the 3D segmentation tool (Mimics Innovation Suite 24, Materialize, Plymouth, MI, US) used in this study is not a standard clinical instrument utilized in everyday clinical practice, and its availability is low. However, the MAD may be also easily detected using standard multiplanar reconstructions.

CONCLUSIONS

Cardiac CT may be easily used to accurately detect and evaluate MADs. Three-dimensional CT reconstructions allow examination of the entire circumference of the mitral annulus and therefore make it a suitable imaging modality to visualize disjunctions, minimizing the likelihood of MAD misdiagnosis. In our study population, a-MAD was identified in 25.6% of cases, v-MAD in 27.6%, with the remaining 46.8% exhibiting a standard aligned annular junction. MADs were typically sectional and did not extend beyond one of the mural mitral leaflet scallop or commissures, with the P2 scallop being the most frequent site for both a-MAD and v-MAD. The commissural MADs were significantly smaller than mural leaflet MADs. Given these findings, further research is essential to elucidate the clinical implications of a-MADs and v-MADs.

Article information

Conflict of interest: None declared.

Funding: None.

REFERENCES

1. Krawczyk-Ożóg A, Batko J, Zdzierak B, et al. Morphology of the mural and commissural atrioventricular junction of the mitral valve. Heart. 2024; 110(7): 517–522, doi: 10.1136/heartjnl-2023-322965, indexed in Pubmed: 37935571.
2. Anderson RH, Garbi M, Zugwitz D, et al. Anatomy of the mitral valve relative to controversies concerning the so-called annular disjunction. Heart. 2023; 109(10): 734–739, doi: 10.1136/heartjnl-2022-322043, indexed in Pubmed: 36585240.
3. Anderson RH, Westaby J, Sheppard MN, et al. Mitral annular disjunction: a ubiquitous finding with or without mitral valvar prolapse. Heart. 2024; 110(7): 463–465, doi: 10.1136/heartjnl-2023-323501, indexed in Pubmed: 38000898.
4. Krawczyk-Ożóg A, Hołda MK, Batko J, et al. Description and prevalence of ventricular mitral annular disjunction: variation of normality or pathological variant? Rev Esp Cardiol (Engl Ed). 2024 [Epub ahead of print], doi: 10.1016/j.rec.2024.04.003, indexed in Pubmed: 38641167.
5. Henle J. Handbuch der systematischen Anatomie des Menschen. Vol. 3. Vieweg, 1876 : 14–20.
6. Hutchins GM, Moore GW, Skoog DK. The association of floppy mitral valve with disjunction of the mitral annulus fibrosus. N Engl J Med. 1986; 314(9): 535–540, doi: 10.1056/NEJM198602273140902, indexed in Pubmed: 3945291.
7. Bennett S, Thamman R, Griffiths T, et al. Mitral annular disjunction: A systematic review of the literature. Echocardiography. 2019; 36(8): 1549–1558, doi: 10.1111/echo.14437, indexed in Pubmed: 31385360.
8. Konda T, Tani T, Suganuma N, et al. The analysis of mitral annular disjunction detected by echocardiography and comparison with previously reported pathological data. J

Echocardiogr. 2017; 15(4): 176–185, doi: 10.1007/s12574-017-0349-1, indexed in Pubmed: 28799132.

9. Krawczyk-Ożóg A, Chyrchel B, Hołda MK, et al. Biannular atrioventricular valve disjunction as a potential cause of ventricular remodeling and subsequent cardiac arrest. Kardiol Pol. 2024 [Epub ahead of print], doi: 10.33963/v.phj.101132, indexed in Pubmed: 38887783.
10. Lee APW, Jin CN, Fan Y, et al. Functional implication of mitral annular disjunction in mitral valve prolapse: A quantitative dynamic 3D echocardiographic study. JACC Cardiovasc Imaging. 2017; 10(12): 1424–1433, doi: 10.1016/j.jcmg.2016.11.022, indexed in Pubmed: 28528161.
11. Perazzolo Marra M, Basso C, De Lazzari M, et al. Morphofunctional abnormalities of mitral annulus and arrhythmic mitral valve prolapse. Circ Cardiovasc Imaging. 2016; 9(8): e005030, doi: 10.1161/CIRCIMAGING.116.005030, indexed in Pubmed: 27516479.
12. Dejgaard LA, Skjølsvik ET, Lie ØH, et al. The mitral annulus disjunction arrhythmic syndrome. J Am Coll Cardiol. 2018; 72(14): 1600–1609, doi: 10.1016/j.jacc.2018.07.070, indexed in Pubmed: 30261961.
13. Clavel M, Hourdain J, Deharo J, et al. Mitral valve prolapse phenotypes associated with sudden cardiac death. Can J Cardiol. 2015; 31(10): S159–S160, doi: 10.1016/j.cjca.2015.07.342.
14. Essayagh B, Sabbag A, Antoine C, et al. The mitral annular disjunction of mitral valve prolapse: Presentation and outcome. JACC Cardiovasc Imaging. 2021; 14(11): 2073–2087, doi: 10.1016/j.jcmg.2021.04.029, indexed in Pubmed: 34147457.
15. Sabbag A, Essayagh B, Barrera JD, et al. EHRA expert consensus statement on arrhythmic mitral valve prolapse and mitral annular disjunction complex in collaboration with the ESC Council on valvular heart disease and the European Association of Cardiovascular Imaging endorsed cby the Heart Rhythm Society, by the Asia Pacific Heart Rhythm Society, and by the Latin American Heart Rhythm Society. Europace. 2022; 24(12): 1981–2003, doi: 10.1093/europace/euac125, indexed in Pubmed: 35951656.
16. Esposito A, Gatti M, Trivieri MG, et al. Imaging for the assessment of the arrhythmogenic potential of mitral valve prolapse. Eur Radiol. 2024; 34(7): 4243–4260, doi: 10.1007/s00330-023-10413-9, indexed in Pubmed: 38078997.
17. Jaworski K, Firek B, Syska P, et al. Malignant arrhythmia associated with mitral annular

disjunction: Myocardial work as a potential tool in the search for a substrate. Kardiol Pol. 2022; 80(1): 93–94, doi: 10.33963/KP.a2021.0127, indexed in Pubmed: 34643257.
18. Eriksson MJ, Bitkover CY, Omran AS, et al. Mitral annular disjunction in advanced myxomatous mitral valve disease: Echocardiographic detection and surgical correction. J Am Soc Echocardiogr. 2005; 18(10): 1014–1022, doi: 10.1016/j.echo.2005.06.013, indexed in Pubmed: 16198877.
19. Carmo P, Andrade MJ, Aguiar C, et al. Mitral annular disjunction in myxomatous mitral valve disease: A relevant abnormality recognizable by transthoracic echocardiography. Cardiovasc Ultrasound. 2010; 8: 53, doi: 10.1186/1476-7120-8-53, indexed in Pubmed: 21143934.
20. Wunderlich NC, Ho SY, Flint N, et al. Myxomatous mitral valve disease with mitral valve prolapse and mitral annular disjunction: Clinical and functional significance of the coincidence. J Cardiovasc Dev Dis. 2021; 8(2): 9, doi: 10.3390/jcdd8020009, indexed in Pubmed: 33498935.
21. Putnam AJ, Kebed K, Mor-Avi V, et al. Prevalence of mitral annular disjunction in patients with mitral valve prolapse and severe regurgitation. Int J Cardiovasc Imaging. 2020; 36(7): 1363–1370, doi: 10.1007/s10554-020-01818-4, indexed in Pubmed: 32221771.
22. Tsianaka T, Matziris I, Kobe A, et al. Mitral annular disjunction in patients with severe aortic stenosis: Extent and reproducibility of measurements with computed tomography. Eur J Radiol Open. 2021; 8: 100335, doi: 10.1016/j.ejro.2021.100335, indexed in Pubmed: 33748350.
23. Toh H, Mori S, Izawa Yu, et al. Prevalence and extent of mitral annular disjunction in structurally normal hearts: comprehensive 3D analysis using cardiac computed tomography. Eur Heart J Cardiovasc Imaging. 2021; 22(6): 614–622, doi: 10.1093/ehjci/jeab022, indexed in Pubmed: 33713105.
24. Zugwitz D, Fung K, Aung N, et al. Mitral annular disjunction assessed using CMR imaging: Insights from the UK biobank population study. JACC Cardiovasc Imaging. 2022; 15(11): 1856–1866, doi: 10.1016/j.jcmg.2022.07.015, indexed in Pubmed: 36280553.
25. Konda T, Tani T, Suganuma N, et al. Mitral annular disjunction in patients with primary severe mitral regurgitation and mitral valve prolapse. Echocardiography. 2020; 37(11): 1716–1722, doi: 10.1111/echo.14896, indexed in Pubmed: 33091171.
26. Krawczyk-Ożóg A, Hołda MK, Batko J, et al. Three-dimensional cardiac computed

tomography compared with autopsied material for the assessment of the mitral valve. Clin Anat. 2023; 36(2): 250–255, doi: 10.1002/ca.23967, indexed in Pubmed: 36271778.

27. Krawczyk-Ożóg A, Hołda MK, Sorysz D, et al. Morphologic variability of the mitral valve leaflets. J Thorac Cardiovasc Surg. 2017; 154(6): 1927–1935, doi: 10.1016/j.jtcvs.2017.07.067, indexed in Pubmed: 28893395.
28. Newcomb AE, David TE, Lad VS, et al. Mitral valve repair for advanced myxomatous degeneration with posterior displacement of the mitral annulus. J Thorac Cardiovasc Surg. 2008; 136(6): 1503–1509, doi: 10.1016/j.jtcvs.2008.05.059, indexed in Pubmed: 19114198.
29. Verbeke J, Demolder A, De Backer J, et al. Mitral annular disjunction: Associated pathologies and clinical consequences. Curr Cardiol Rep. 2022; 24(12): 1933–1944, doi: 10.1007/s11886-022-01806-1, indexed in Pubmed: 36331783.
30. Drescher CS, Kelsey MD, Yankey GS, et al. Imaging considerations and clinical implications of mitral annular disjunction. Circ Cardiovasc Imaging. 2022; 15(9): e014243, doi: 10.1161/CIRCIMAGING.122.014243, indexed in Pubmed: 36126123.
31. Essayagh B, Iacuzio L, Civaia F, et al. Mitral annular disjunction in mitral valve prolapse: A cardiac magnetic resonance study. Arch Cardiovasc Dis Suppl. 2019; 11(1): 62–63, doi: 10.1016/j.acvdsp.2018.10.136.
32. Blanke P, Dvir D, Cheung A, et al. A simplified D-shaped model of the mitral annulus to facilitate CT-based sizing before transcatheter mitral valve implantation. J Cardiovasc Comput Tomogr. 2014; 8(6): 459–467, doi: 10.1016/j.jcct.2014.09.009, indexed in Pubmed: 25467833.
33. Lin E, Alessio A. What are the basic concepts of temporal, contrast, and spatial resolution in cardiac CT? J Cardiovasc Comput Tomogr. 2009; 3(6): 403–408, doi: 10.1016/j.jcct.2009.07.003, indexed in Pubmed: 19717355.
34. Faletra FF, Leo LA, Paiocchi VL, et al. Morphology of mitral annular disjunction in mitral valve prolapse. J Am Soc Echocardiogr. 2022; 35(2): 176–186, doi: 10.1016/j.echo.2021.09.002, indexed in Pubmed: 34508838.

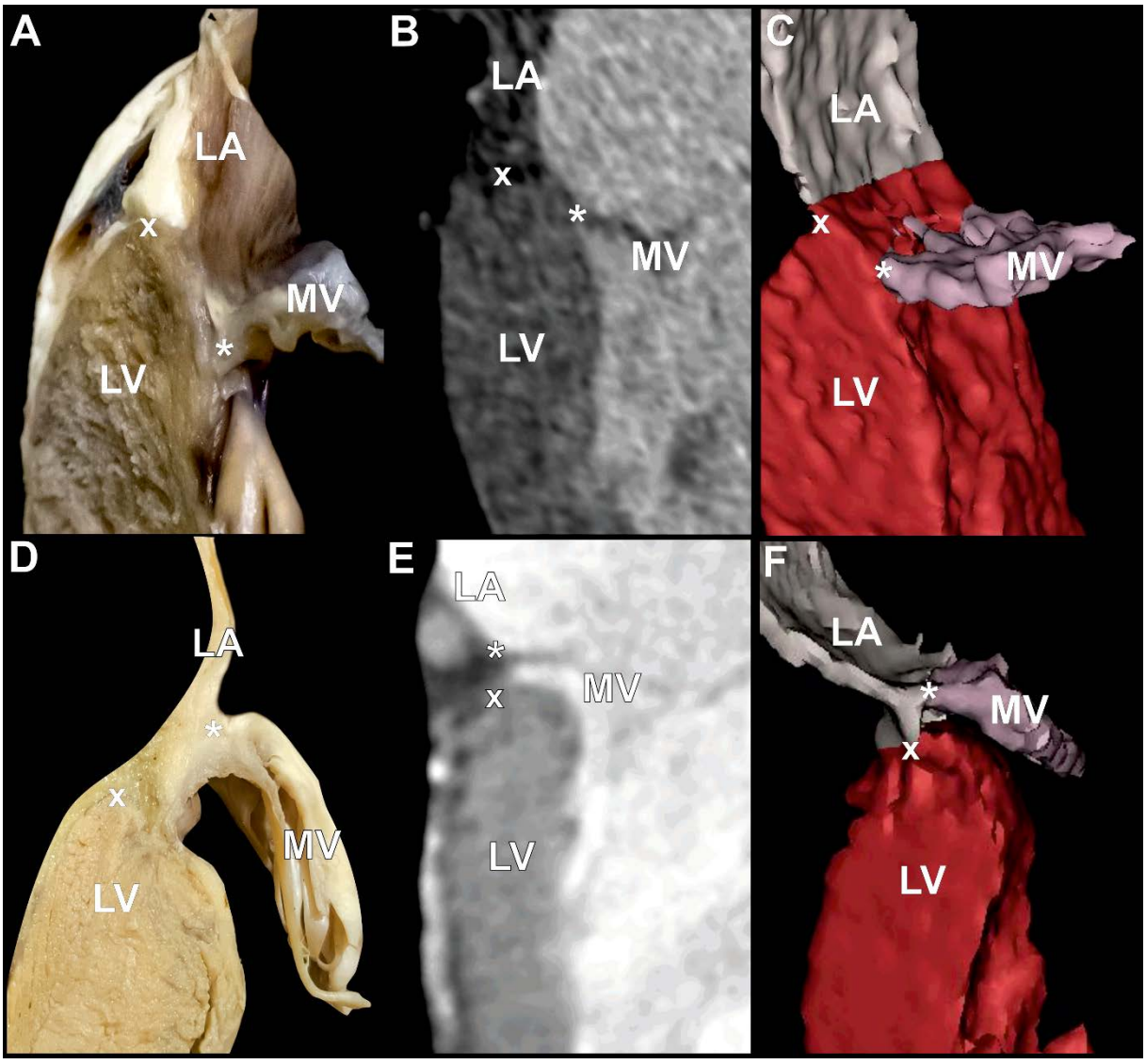

Figure 1. Two types of mitral annular disjunction. **A., D.** Photographs of autopsy hearts specimens showing longitudinal sections through the atrial wall-mitral annulus-ventricular wall junction. **A.** Ventricular mitral annular disjunction type with visible spatial displacement of the mitral leaflet hinge line (asterisk) towards the left ventricle (LV); d: atrial mitral annular disjunction type with visible spatial displacement of the mitral leaflet hinge line towards the left atrium (LA). **B.** Ventricular mitral annular disjunction in 2D (end-systole) in contrast-enhanced computed tomography. **C.** Ventricular mitral annular disjunction in 3D reconstructions (end-systole) segmented from contrast-enhanced computed tomography (Mimics Innovation Suite 24, Materialize). **E.** Atrial mitral annular disjunction in 2D (end-systole) in contrast-enhanced computed tomography. **F.** Atrial mitral annular disjunction in 3D reconstructions (end-systole) segmented from contrast-enhanced computed tomography (Mimics Innovation Suite 24, Materialize)

Abbreviations: MV, mitral valve; x, highest point of the left ventricle myocardium

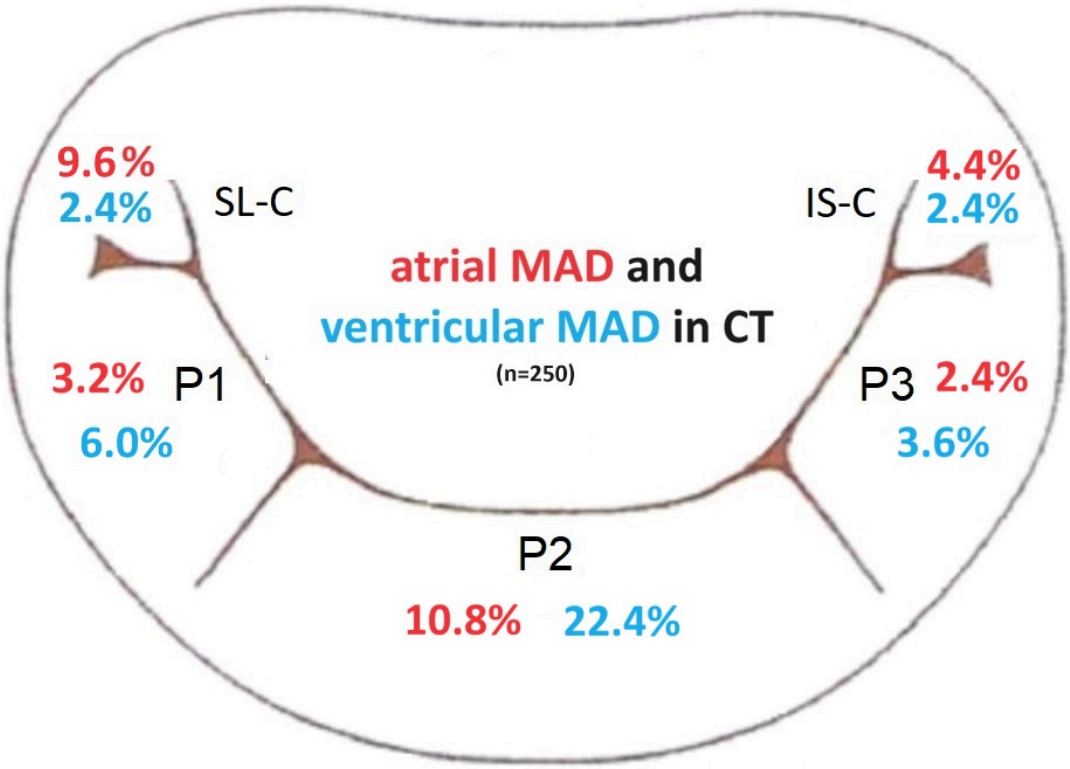

Figure 2. Schematic distribution of atrial and ventricular mitral annular disjunctions (MADs) within the mural mitral leaflet scallops (P1, P2, and P3) and mitral commissures (superolateral commissure (SL-C) and inferoseptal commissure (IS-C)) in the whole studied population (n = 250) detected using computed tomography imaging (CT)

Table 1. Distribution and morphological characteristics of mitral annular disjunction (MAD) types within the mural mitral leaflet and mitral commissures

Mural mitral leaflet		
	Atrial MAD	**Ventricular MAD**
Total, n (%)	29 (11.6)	57 (22.8)
Only in P1 scallop, n (%)	1 (3.4)	0 (0.0)
Only in P2 scallop, n (%)	20 (69.0)	36 (63.2)
Only in P3 scallop, n (%)	1 (3.4)	1 (1.8)
Both in P1 and P2 scallops, n (%)	3 (10.3)	14 (24.6)
Both in P2 and P3 scallops, n (%)	2 (6.9)	5 (8.8)
In all scallops (P1, P2 and P3), n (%)	2 (6.9)	1 (1.8)

Disjunction height, mm, median (IQR)	5.0 (2.8–8.2)	5.3 (3.2–7.0)
Disjunction length, mm, median (IQR)	10.1 (7.1–12.3)	12.9 (8.7–14.9)
Mitral commissures		
Total, n (%)	32 (12.8)	10 (4.0)
In superolateral commissure, n (%)	22 (68.8)	6 (60.0)
In inferoseptal commissure, n (%)	10 (31.3)	4 (40.0)
Disjunction height, mm, median (IQR)	2.9 (2.2–3.4)	3.1 (2.5–4.1)
Disjunction length, mm, median (IQR)	3.7 (2.8–6.2)	4.7 (3.3–6.5)
Mural mitral leaflet and commissures		
Total, n (%)	3 (1.2)	2 (0.8)
In P1 scallop and superolateral commissure, n (%)	2 (66.7)	0 (0.0)
In P3 scallop and inferoseptal commissure, n (%)	1 (33.3)	2 (100)

Abbreviations: IQR, interquartile range; n, number; P1, P2, P3, scallops of mural mitral valve leaflet; SD, standard deviation

Table 2. Prevalence and morphological characteristics of mitral annular disjunctions (MAD) types according to sex

		Males (n = 107)	Females (n = 143)	*P*-value
Atrial MAD	Total, n (%)	28 (26.2)	36 (25.2)	0.86
	Disjunction height, mm, median (IQR)	5.6 (2.9–8.2)	4.1 (2.8–6.6)	0.52
	Disjunction length, mm, median (IQR)	11.4 (10.1–13.7)	7.7 (6.6–11.5)	0.02
Ventricular MAD	Total, n (%)	33 (30.8)	36 (25.2)	0.32
	Disjunction height, mm, median (IQR)	6.2 (4.1–7.0)	4.5 (3.0–6.6)	0.16
	Disjunction length, mm, median (IQR)	13.0 (9.7–17.2)	12.1 (7.6–14.5)	0.30

Abbreviations: see Table 1

Table 3. Clinical characteristic of the patients according to the detected type of the mitral annular disjunction (MAD).

	No-MAD (n = 117)	Atrial MAD (n = 64)	Ventricular MAD (n = 69)	*P*-value ANOVA	Pairwise comparisons		
					P-value atrial MAD vs. no-MAD	*P*-value ventricular MAD vs. no-MAD	*P*-value atrial MAD vs. ventricular MAD
Age, years, mean (SD)	75.8 (13.7)	68.5 (17.2)	75.8 (12.4)	0.006	0.003	0.41	0.02
Females, n (%)	71 (60.7)	36 (56.3)	36 (52.2)	–	0.56	0.26	0.64
Body mass index, kg/m^2, mean (SD)	27.2 (4.6)	27.2 (4.8)	27.3 (4.4)	0.72	–	–	–
Body surface area, m^2, mean (SD)	1.8(0.2)	1.8 (0.3)	1.8 (0.2)	0.45	–	–	–
Arterial hypertension, n (%)	92 (81.4)	50 (80.6)	56 (81.2)	–	0.90	0.97	0.94
Atrial fibrillation, n (%)	38 (33.6)	20 (32.3)	25 (36.2)	–	0.85	0.72	0.63
Diabetes mellitus type II, n (%)	38 (33.6)	21 (33.9)	18 (26.1)	–	0.97	0.29	0.33
Chronic kidney disease, n (%)	26 (23.0)	9 (14.5)	17 (25)	–	0.18	0.76	0.14
Coronary artery disease, n (%)	61 (52.1)	26 (40.6)	37 (53.6)	–	0.14	0.85	0.13
Previous myocardial infarction, n (%)	32 (28.3)	12 (19.4)	26 (37.7)	–	0.19	0.19	0.02
Chronic obstructive pulmonary disease, n (%)	10 (8.8)	3 (4.8)	6 (8.7)	–	0.39	0.97	0.38
Previous stroke or transient ischemic attack, n (%)	15 (13.3)	5 (8.1)	7 (10.1)	–	0.30	0.53	0.68
Presence of pacemaker, n (%)	8 (7.1)	4 (6.5)	7 (10.1)	–	0.88	0.47	0.45

Ever-smoker, n (%)		28 (24.8)	15 (24.2)	17 (24.6)	–	0.93	0.98	0.95
Cardiac arrest, n (%)		1 (0.9)	1 (1.6)	1 (1.5)	–	0.66	0.70	0.97
Severe aortic valve stenosis, n (%)		87 (74.4)	30 (46.9)	51 (73.9)	–	<0.001	0.95	0.001
Severe aortic valve regurgitation, n (%)		0 (0)	2 (3.1)	1 (1.4)	–	0.12	0.37	0.61
Mitral valve regurgitation, n (%)	Severe	1 (0.9)	2 (3.1)	4 (5.8)	–	0.25	0.04	0.45
	Moderate	22 (18.8)	12 (18.8)	21 (30.4)	–	0.99	0.07	0.07
	Mild	65 (55.6)	29 (45.3)	30 (43.5)	–	0.19	0.11	0.83
	None/trivial	29 (24.8)	21 (32.8)	14 (20.3)	–	0.25	0.48	0.10
Barlow syndrome, n (%)		0	1 (1.6)	0 (0)	–	0.18	–	0.30
Left ventricle ejection fraction, %, mean (SD)		53.4 (12.1)	56.9 (10.1)	53.7 (13.6)	0.36	–	–	–

Abbreviations: see Table 1